AIP | The Journal of Chemical Physics

Spectroscopic study on deuterated benzenes. II. High-resolution laser spectroscopy and rotational structure in the S1 state

Sachi Kunishige, Toshiharu Katori, Masaaki Baba, Masato Hayashi, Hirokazu Hasegawa, and Yasuhiro Ohshima

Citation: The Journal of Chemical Physics **143**, 244303 (2015); doi: 10.1063/1.4937950
View online: http://dx.doi.org/10.1063/1.4937950
View Table of Contents: http://scitation.aip.org/content/aip/journal/jcp/143/24?ver=pdfcov
Published by the AIP Publishing

Spectroscopic study on deuterated benzenes. II. High-resolution laser spectroscopy and rotational structure in the S_1 state

Sachi Kunishige,[1] Toshiharu Katori,[1] Masaaki Baba,[1,a)] Masato Hayashi,[2] Hirokazu Hasegawa,[3] and Yasuhiro Ohshima[2,4]
[1]*Division of Chemistry, Graduate School of Science, Kyoto University, Kyoto 606-8502, Japan*
[2]*Institute for Molecular Science, National Institute of Natural Science, Myodaiji, Okazaki 444-8585, Japan*
[3]*Department of Basic Science, Graduated School of Arts and Sciences, The University of Tokyo, Meguro-ku, Tokyo 153-8902, Japan*
[4]*Department of Chemistry, Graduate School of Science and Engineering, Tokyo Institute of Technology, Ohokayama, Meguro-ku, Tokyo 152-8551, Japan*

(Received 14 September 2015; accepted 2 December 2015; published online 23 December 2015)

High-resolution spectra of the $S_1 \leftarrow S_0$ transition in jet-cooled deuterated benzenes were observed using pulse dye amplification of single-mode laser light and mass-selective resonance enhanced multiphoton ionization (REMPI) detection. The vibrational and rotational structures were accurately analyzed for the vibronic levels in the S_1 state. The degenerate 6^1 levels of C_6H_6 or C_6D_6 are split into $6a^1$ and $6b^1$ in many of deuterated benzenes. The rigid-rotor rotational constants were assessed and found to be slightly different between 6a and 6b because of different mean molecular structures. Their rotational levels are significantly shifted by Coriolis interactions. It was found that the Coriolis parameter proportionally changed with the number of substituted D atoms. © *2015 AIP Publishing LLC.* [http://dx.doi.org/10.1063/1.4937950]

I. INTRODUCTION

The electronic excited states of benzene are of great interest and extensive studies using various spectroscopic methods have been performed.[1–4] In Paper I, we showed that the benzene molecule was a planar regular hexagon (D_{6h}) and the structure was not changed by deuterium substitution.[5] In the electronic excited state, the mean molecular structure is easily varied with adiabatic and non-adiabatic interactions. High-resolution spectroscopy is powerful for investigating such interactions and excited-state dynamics. In Paper II, we discuss the vibrational and rotational level structures of deuterated benzenes. In particular, we focus on the degenerate ν_6 (e_{2g}) mode of C_6H_6 which splits into ν_{6a} and ν_{6b} for deuterated benzenes of lower symmetry. The degenerate $6^1(e_{2g})$ levels split into two levels of different symmetries, $6a^1$ and $6b^1$, in some isotopomers. It is very important to investigate systematically the vibrational and rotational structures because they vary depending on the isotopomer. The rotational structures of C_6H_6 and C_6D_6 have been completely analyzed by Sieber *et al.*[6] and Okruss *et al.*[7] by high-resolution laser spectroscopy. As for the partially substituted isotopomer, there has been no report other than the work on C_6H_5D by Riedle *et al.*[8]

C_6H_6 is a planar regular hexagon (D_{6h}) and possesses 10 types of degenerate vibrations.[9,10] Although the $S_1\ ^1B_{2u} \leftarrow S_0\ ^1A_{1g}$ transition is forbidden, the vibronic bands are observed by intensity-borrowing from other electronic states.[11] Ultrahigh-resolution spectra ($\Delta E = 0.0001\ cm^{-1}$) of the S_1–S_0 vibronic bands were already observed for C_6H_6 and C_6D_6, and the rotational constants and Coriolis parameter were accurately determined using a least-squares fit of a large number of spectral lines.[6,7,12–14] For deuterated benzenes, we performed high-resolution spectroscopy with narrow-band pulsed laser light ($\Delta E = 0.005\ cm^{-1}$), which was obtained by pulse dye amplification of single-mode cw laser light. We identified the 6_0^1 (or $6a_0^1$ and $6b_0^1$) bands of every H/D isotopomer, and determined the rigid-rotor rotational constants in the excited state. Coriolis interaction shifts the rotational levels of these degenerate or near-degenerate vibrational levels. We discuss the Coriolis parameter determined by a least-squares fit of observed spectral lines.

II. EXPERIMENTAL

The mixed sample of deuterated benzenes is the same as that used in Paper I.[5] Here, we briefly describe the experimental setup because the details were described previously.[15,16] We generated a supersonic jet with He gas at the stagnation pressure of 70 atm. The rotational temperature was estimated to be about 1 K. The jet was collimated using a conical skimmer and crossed with a laser beam at right angles in an ionization chamber. As a source of exciting light, we used a cw single-mode Ti:sapphire laser (Spectra Physics, Matisse TROB2-W, $\Delta E = 0.0001\ cm^{-1}$) pumped by a Nd^{3+}:YVO_4 laser (Spectra Physics, Millennia 10sJs). The output was pulse dye amplified using a pulsed laser (Spectra Physics LAB-190-10, 532 nm, $\Delta t = 5$ ns). The third harmonics was generated to excite the deuterated benzene molecules. In addition, we used a pulsed dye laser (Continuum ND6000JST, $\Delta E = 0.3\ cm^{-1}$) pumped by a pulsed Nd^{3+}:YAG laser (Continuum, SureliteII-10, 355 nm) to ionize the excited molecules. The $C_6H_{6-N}D_N^+$ ion was detected by a microchannel plate (MCP) detector (Galileo) through a time-of-flight tube. The transient MCP

a)Author to whom correspondence should be addressed. Electronic mail: baba@kuchem.kyoto-u.ac.jp

signal output was recorded by changing the wavelength of exciting laser light. The mass-selective resonance enhanced multiphoton ionization (REMPI) excitation spectrum was obtained by gating the signal at an appropriate flight time. The absolute wavelength of the exciting laser light was calibrated using a wavemeter (High Finesse WS-7).

III. RESULTS AND DISCUSSION

A. Spectral analysis

1. C_6H_5D

The top of Fig. 1 illustrates a REMPI excitation spectrum detected at the mass-to-charge ratio $m/e = 79$. Two bands were separately observed with the split of approximately 3 cm^{-1}. These are two components of the degenerate vibrational levels of $v_6(e_{2g}) = 1$ in C_6H_6, which are split because symmetry is reduced in C_6H_5D. Similar spectra were already reported by Riedle *et al.*[8] Only a small number of rotational lines are seen because the rotational temperature is very low in this setup. However, it is difficult to accurately determine the high-order terms such as centrifugal distortion constants. We, therefore, analyzed the spectra using the following Hamiltonian of a vibrating-rotating molecule with a harmonic vibrator, rigid-rotor, and vibrational angular momentum terms[17]

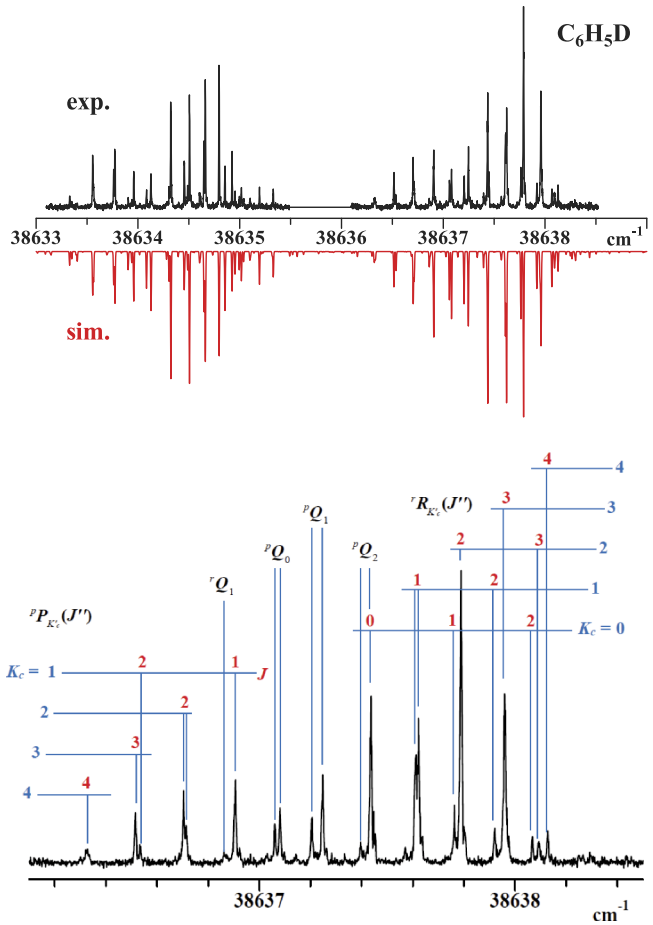

FIG. 1. REMPI excitation spectra of $6a^1$ and $6b^1$ bands of C_6H_5D and assignments of the rotational lines for the $6a^1$ band.

$$H = \frac{(J_x - P_x)^2}{2I_x} + \frac{(J_y - P_y)^2}{2I_y} + \frac{(J_z - P_z)^2}{2I_z} + \frac{1}{2}\sum_r (P_r^2 + \lambda_r Q_r^2). \quad (1)$$

Here Q_r and P_r are a typical normal coordinate and its conjugate momentum, respectively. λ_r is the force constant. Eq. (1) includes Coriolis interaction, which will be discussed in detail in Section III C. Although C_6H_5D is an asymmetric top (rigid rotor rotational constants $A \neq B \neq C$), the spectral feature is similar to that of an oblate symmetric top ($A = B > C$). The rotational transition is represented by ${}^{\Delta K_c}\Delta J_{K_c''}(J'')$, where J and K_c are the quantum numbers of total angular momentum and its c-axis component, respectively. c is the principal axis, which is perpendicular to the molecular plane of benzene. The $\pi\pi^*$ transition moment is perpendicular to this c axis, and the selection rules are $\Delta J = 0, \pm 1$ and $\Delta K_c = \pm 1$. As shown at the bottom of Fig. 1, the main lines are assigned to ${}^pR_{K_c''}(J'')$, ${}^rR_{K_c''}(J'')$, ${}^pQ_{K_c''}(J'')$, ${}^rQ_{K_c''}(J'')$, ${}^pP_{K_c''}(J'')$, and ${}^rP_{K_c''}(J'')$.

The rotational constants in the ground state were accurately determined by Oldani and Bauder.[18] Although we also determined these values using the mean molecular structure, which is given in Paper I,[5] our values were almost identical to their values. In this spectral analysis, we used our values and determined the rotational constants at the 6a and 6b vibrational levels in the S_1 state by a least-squares fit using the PGOPHER program.[19] The resultant values are tabulated in Table I. The rotational constants were found to be slightly different between 6a and 6b. The normal coordinates are illustrated in Fig. 2. The mean molecular structures are expected to be different in these two levels because the mean bond lengths are generally larger than the equilibrium bond lengths because of anharmonicity.[20,21]

It is difficult to accurately estimate the molecular structure and vibrational energies of 6a and 6b. We therefore identified these bands referring to the results of theoretical calculations using the Gaussian 09 program package.[22] For all isotopomers, we calculated vibrational energies of v_6 by TDDFT(B3LYP)/6-31++G(d,p) without considering anharmonicity. The resultant energies are scaled by 0.983. The calculations indicated that the 6a vibrational energy was about 3 cm^{-1} smaller than 6b.

2. $C_6H_4D_2$

The high-resolution spectra of $C_6H_4D_2$ ($m/e = 80$) are shown in Fig. 3. We found three series of 6a and 6b bands with the splits of about 2.2 and 5 cm^{-1}, respectively. There are three isotopomers for $C_6H_4D_2$, which are expressed as *ortho*, *meta*, and *para* (Fig. 2). The results of theoretical calculations for band splitting were 2.0, 2.0, and 5.3 cm^{-1}, respectively. The band observed in the higher energy region around 38 669 cm^{-1} is easily identified to originate from *p*-$C_6H_4D_2$. Two other series are mostly overlapped in the same energy region. We assigned their rotational lines by referring to the calculated rotational constants for *o*-$C_6H_4D_2$ and *m*-$C_6H_4D_2$. Part of the expanded spectrum is shown with the assignments at the bottom of Fig. 3. The selection rules

TABLE I. Rotational constants (cm^{-1}) in the 6^1 (or $6a^1$ and $6b^1$) levels in the S_1 states of deuterated isotopomers.

	6a				6b				
	A	*B*	*C*	ΔT_0[a]	*A*	*B*	*C*	ΔT_0[a]	$\xi^c_{6a,6b}$
C_6H_6[14]	0.181 790 7(3)	0.181 790 7(3)	0.090 870 33(13)						0.105 130 2(3)
C_6H_5D	0.181 89(4)	0.170 01(4)	0.087 91(1)	28.138 3(1)	0.181 41(4)	0.170 45(3)	0.087 90(1)	31.0736(1)	0.096 2(1)
o-$C_6H_4D_2$	0.176 05(9)	0.165 39(7)	0.085 08(2)	60.722 9(3)	0.176 54(7)	0.165 10(8)	0.085 19(3)	57.9291(4)	0.087 9(3)
m-$C_6H_4D_2$	0.175 77(6)	0.165 33(6)	0.085 02(2)	60.493 7(3)	0.175 84(4)	0.165 12(5)	0.085 23(2)	57.8223(3)	0.087 9(2)
p-$C_6H_4D_2$	0.181 80(9)	0.160 9(1)	0.085 08(2)	56.806 8(3)	0.182 14(8)	0.159 88(6)	0.085 15(2)	62.6507(3)	0.087 8(5)
1,3,5-$C_6H_3D_3$	0.165 466(4)	0.165 466(4)	0.082 433(2)	88.965 7(1)					0.077 74(1)
1,2,3-$C_6H_3D_3$	0.165 7(3)	0.165 3(3)	0.081 8(4)	88.847 1(3)	0.165 6(2)	0.165 3(2)	0.083 3(4)	88.8191(3)	0.078 38(4)
1,2,4-$C_6H_3D_3$	0.174 4(1)	0.156 82(7)	0.082 46(2)	87.090 6(3)	0.174 42(8)	0.156 76(6)	0.082 45(3)	91.7545(3)	0.080 0(4)
o-$C_6H_2D_4$	0.165 22(9)	0.155 6(1)	0.080 13(4)	117.793 7(5)	0.165 5(1)	0.155 2(1)	0.080 06(4)	120.3938(4)	0.072 7(5)
m-$C_6H_2D_4$	0.165 82(9)	0.155 9(1)	0.080 09(3)	117.714 2(5)	0.165 1(1)	0.156 1(1)	0.079 94(4)	120.4061(4)	0.072 6(5)
p-$C_6H_2D_4$	0.169 9(2)	0.151 2(2)	0.079 98(3)	122.130 7(5)	0.171 2(3)	0.150 2(3)	0.079 84(6)	117.2752(6)	0.072 6(8)
C_6HD_5	0.160 32(2)	0.151 31(2)	0.077 595(5)	150.564 03(8)	0.160 49(2)	0.151 61(2)	0.077 608(5)	148.1985(1)	0.065 67(6)
C_6D_6	0.151 107 2(2)	0.151 107 2(2)	0.075 412 24(10)	179.837 02(5)					0.059 036 2(4)

[a]ΔT_0 (cm^{-1}) = $T'_0 - T_0$ (C_6H_6) = $T'_0 - 38\,606.1025$. Here, T_0 (C_6H_6) is the rotationless origin of 6^1_0 band of C_6H_6, and T'_0 represents the rotationless band origin of each band.

for rotational transition are identical to those of C_6H_5D. The abundance ratio is considered to be *ortho*:*meta*:*para* = 2:2:1 because the sample mixture (H:D = 1:1) is within the statistical limit distribution after exchange reaction of sufficiently long time.

3. $C_6H_3D_3$

Fig. 4 shows the high-resolution REMPI excitation spectrum of $C_6H_3D_3$ (m/e = 81) and its simulation. We found three series of bands, which correspond to the three isotopomers of $C_6H_3D_3$ shown in Fig. 5. One series was split into two bands with the peaks at 38 693.3 and 38 698.4 cm^{-1}. We performed theoretical calculations of vibrational energies, and the resultant band splits were 0.1, 3.9, and 0 cm^{-1} for 1,2,3-$C_6H_3D_3$, 1,2,4-$C_6H_3D_3$, and 1,3,5-$C_6H_3D_3$, respectively. The above series which has large splitting, therefore, is easily assigned to 1,2,4-$C_6H_3D_3$. The other two series are severely overlapped in the center region, and we could not assign the observed rotational lines. We therefore observed the high-resolution spectrum using the pure sample of 1,3,5-$C_6H_3D_3$. In this case, we reduced the He stagnation pressure (10 atm) to raise the rotational temperature and observe many transitions for high J'' and K'' levels. The result is shown in Fig. 6.

The contour is remarkably different from that of the typical perpendicular band of an oblate symmetric top that results from the energy shift by Coriolis interaction in the upper levels, about 1.0 cm^{-1} in maximum among the observed shifts. The statistical weights of nuclear spin states are tabulated in the Appendix, and we estimated the relative intensities of rotational lines assuming a temperature of 3 K. The simulation shown in Fig. 6 is in good agreement with the observed spectrum. The rotational lines of 1,2,3-$C_6H_3D_3$ could also be assigned because those of 1,3,5-$C_6H_3D_3$ were identified by the above analysis. We thus determined the rotational constants and Coriolis parameters of all $C_6H_3D_3$ isotopomers, which are tabulated in Table I.

B. Band origins and rotational constants

Because the spectral features of $C_6H_2D_4$ and C_6HD_5 were analogous to those of $C_6H_4D_2$ and C_6H_5D, respectively, we did not describe the analysis procedure in detail. We can determine the band origins of $S_1 \leftarrow S_0$ $6a^1_0$ and $6b^1_0$ bands, rigid-rotor rotational constants, and Coriolis parameters for deuterated benzene isotopomers. The results are listed in Table I.

The degenerate 6^1 (e_{2g}) vibrational levels of C_6H_6 split into two different energy levels because of reduced symmetry that results from deuterium substitution. We express them as 6a and 6b, of which the energy difference ΔE_{a-b} is 2-5 cm^{-1}. We define 6a and 6b by the normal coordinates, as shown in Fig. 2. The relative energies depend on the isotopomers. The rotational constants are appreciably different between the 6a and 6b levels. This is attributed to their different mean molecular structures, which depend on the change in bond lengths that results from anharmonicity in the potential energy.[20]

C. Coriolis parameters

Coriolis interactions about the z axis (out of plane) occur on the rotational levels of degenerate ν_6 vibrations or near-degenerate ν_{6a} and ν_{6b} vibrations. We consider an approximate treatment of the experimental results.[17] The vibrational angular momentum about the z axis is generally given by

$$P_z = -\sum_n i\hbar \left[x_n \left(\frac{\partial}{\partial y_n} \right) - y_n \left(\frac{\partial}{\partial x_n} \right) \right], \tag{2}$$

where x_n and y_n are the mass-adjusted Cartesian displacement coordinates of the atom n. They are defined by

$$x_n = \sqrt{m_n}\, X_n, y_n = \sqrt{m_n}\, Y_n, \tag{3}$$

where m_n is the atomic mass. X_n and Y_n are dimensionless parameters, which are the atomic displacement coordinates divided by normal vibrational coordinates. The vibrational

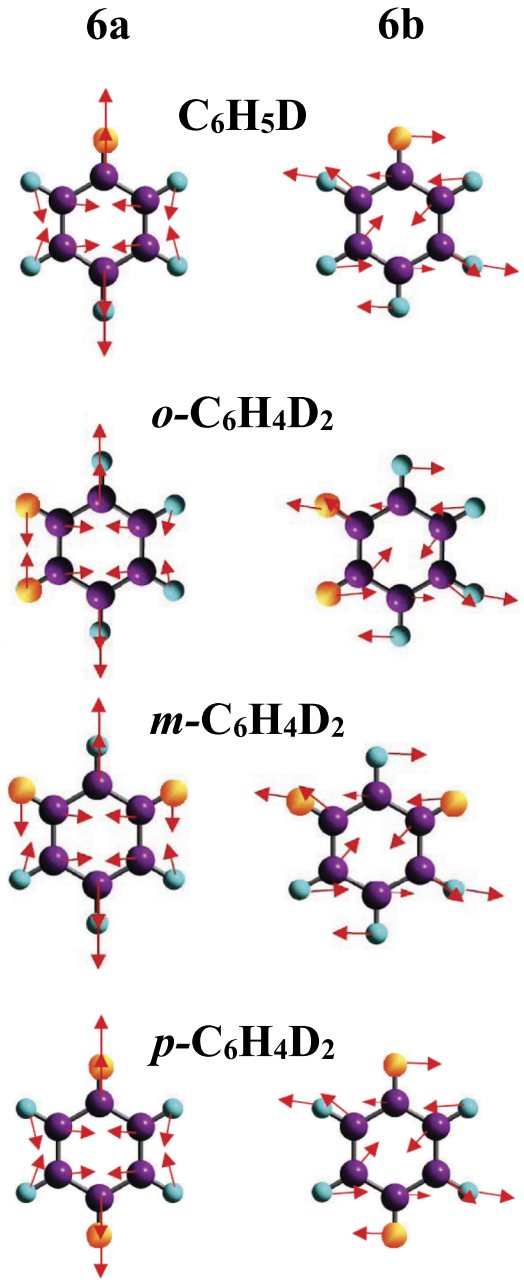

FIG. 2. Normal coordinates of 6a and 6b vibrations of C_6H_5D and three $C_6H_4D_2$ isotopomers.

angular momentum is also expressed in terms of the normal coordinates of r and s modes,

$$P_z = \sum_r \sum_s \zeta^z_{r,s} [Q_r P_s - Q_s P_r]. \quad (4)$$

Although the sums are generally taken over all possible combinations of Q_r and Q_s, only the sums for the combination of Q_{6a} and Q_{6b} were used. The Coriolis zeta constant is defined by

$$\zeta^z_{r,s} = \sum_n \left[\left(\frac{\partial x_n}{\partial Q_r} \right) \left(\frac{\partial y_n}{\partial Q_s} \right) - \left(\frac{\partial x_n}{\partial Q_s} \right) \left(\frac{\partial y_n}{\partial Q_r} \right) \right]. \quad (5)$$

The sign of $\zeta^z_{r,s}$ depends on the choice of sense of Q_r and Q_s, and the order of r and s.

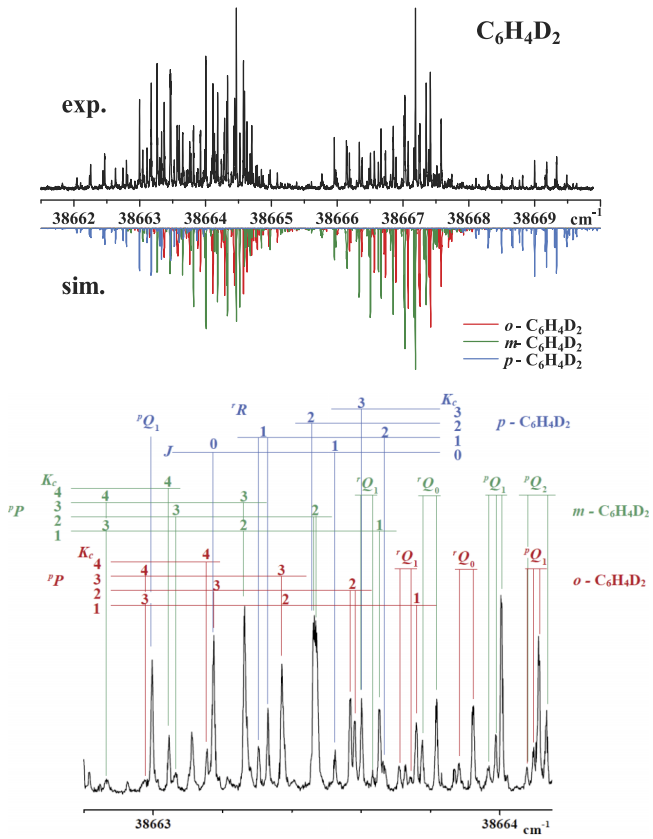

FIG. 3. REMPI excitation spectra of $6a^1$ and $6b^1$ bands of $C_6H_4D_2$, and expanded spectrum and their assignments.

For a pair of normal coordinate of degenerate or near-degenerate vibrational modes 6a and 6b, the Coriolis zeta constant is given by

$$\zeta^z_{6a,6b} = \sum_n \left[\left(\frac{\partial x_n}{\partial Q_{6a}} \right) \left(\frac{\partial y_n}{\partial Q_{6b}} \right) - \left(\frac{\partial x_n}{\partial Q_{6b}} \right) \left(\frac{\partial y_n}{\partial Q_{6a}} \right) \right]. \quad (6)$$

The Hamiltonian (Eq. (1)) consists of three terms

$$H = H_v + H_r + H'. \quad (7)$$

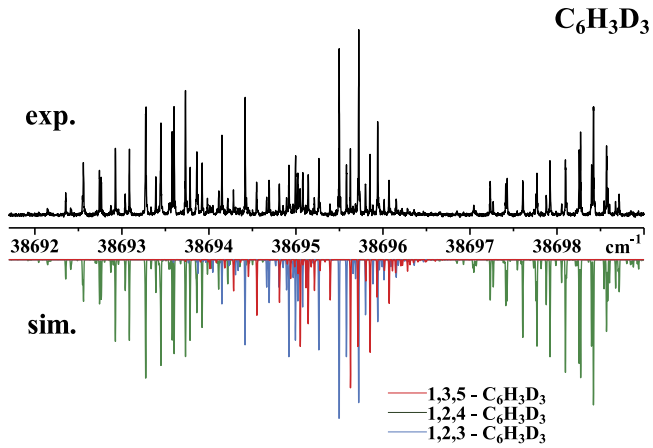

FIG. 4. REMPI excitation spectra of $C_6H_3D_3$.

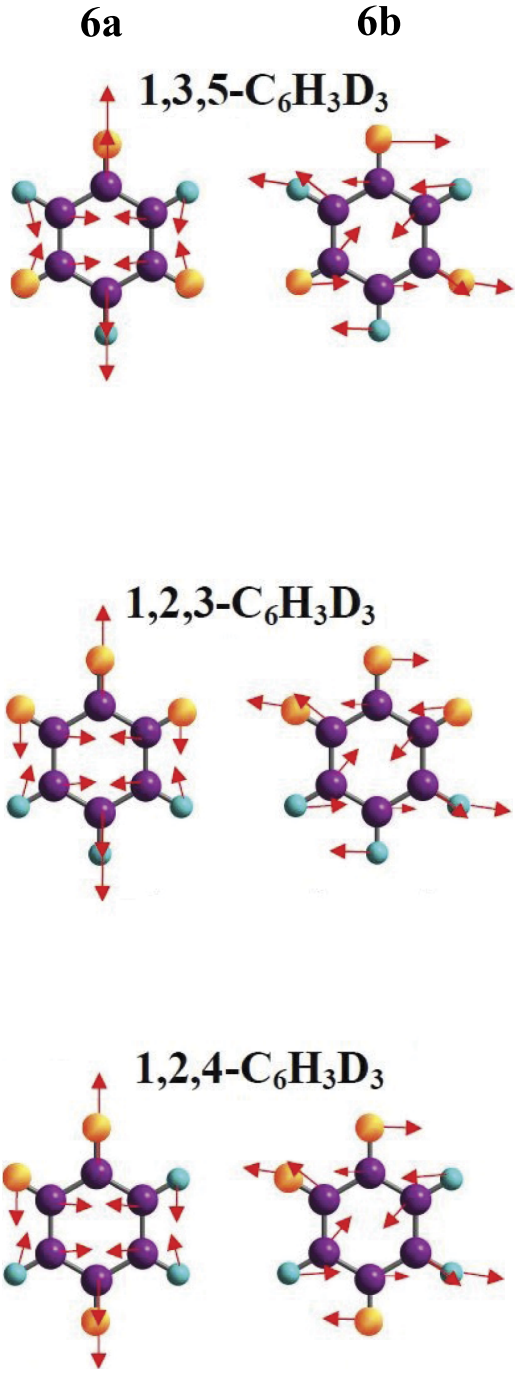

FIG. 5. Normal coordinates of 6a and 6b vibrations of three $C_6H_3D_3$ isotopomers.

H_r is the term on a rigid rotor and is expressed as

$$H_r = \frac{J_x^2}{2I_x} + \frac{J_y^2}{2I_y} + \frac{J_z^2}{2I_z}, \tag{8}$$

where J_x, J_y, and J_z are the components of total angular momentum, and I_x, I_y, and I_z are the moments of inertia. It is also expressed using the rotational constants

$$\begin{aligned} H_r &= AJ_a^2 + BJ_b^2 + CJ_c^2 \\ &= \frac{1}{2}(A+B)J^2 + \left[C - \frac{1}{2}(A+B)\right] J_c^2 \\ &\quad + \frac{1}{4}(A-B)(J_+^2 + J_-^2). \end{aligned} \tag{9}$$

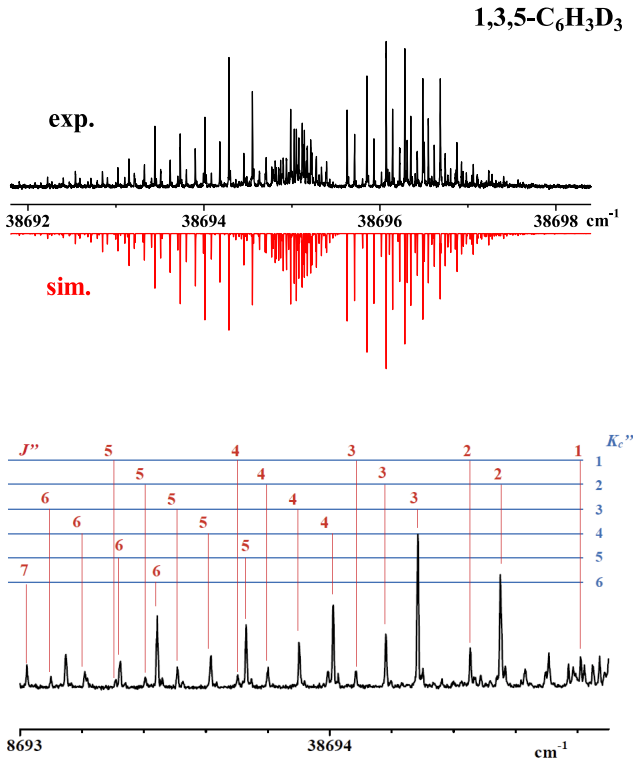

FIG. 6. REMPI excitation spectrum of 1,3,5-$C_6H_3D_3$.

The relationship between the molecular axes x, y, z and the rotational principal axes a, b, c is complicated and depends on the symmetry.

H_v is the term of harmonic vibrations. H' is the term of perturbation involving the vibrational angular momentum and is given by

$$H' = -\frac{P_x J_x}{I_x} - \frac{P_y J_y}{I_y} - \frac{P_z J_z}{I_z} + \frac{P_x^2}{2I_x} + \frac{P_y^2}{2I_y} + \frac{P_z^2}{2I_z}. \tag{10}$$

The Coriolis interaction between 6a and 6b arises from the P_z terms. Assuming that the P_z^2 term is negligibly small, we obtain

$$H' = -\frac{P_z J_z}{I_z} = -2C\ \zeta_{6a,6b}^z\ [Q_{6a}P_{6b} - Q_{6b}P_{6a}]. \tag{11}$$

The experimental Coriolis parameter $\xi_{6a,6b}^c$ for level energy shifts is defined by

$$\xi_{6a,6b}^c = |2C\ \zeta_{6a,6b}^z\ \Omega|. \tag{12}$$

Ω is given by

$$\Omega = \frac{1}{2}\left(\sqrt{\frac{\nu_{6a}}{\nu_{6b}}} + \sqrt{\frac{\nu_{6b}}{\nu_{6a}}}\right) \tag{13}$$

and the value can be estimated to be equal to one.

First we obtained the $\xi_{6a,6b}^c$ value using a least-squares fit of the transition wavenumbers of observed spectral lines for the $6a_0^1$ and $6b_0^1$ bands of deuterated benzenes. In this case, the selection rules of Coriolis interaction about the c axis are $\Delta J = 0$, $\Delta K_c = 0$. The level energies are obtained by diagonalizing the matrix

$$\begin{pmatrix} G(6a^1) + F(J,K_a,K_c) & -i\,\xi^c_{6a,6b}K_c \\ i\,\xi^c_{6a,6b}K_c & G(6b^1) + F(J,K_a,K_c) \end{pmatrix}, \quad (14)$$

where G and F are the vibrational and rotational term values, respectively. K_a is the quantum number of the a-axis component of the total angular momentum. The results are shown in Fig. 7. It can be seen that $\xi^z_{6a,6b}$ proportionally changes with the number of D atoms (N_D).

Here, we consider the atomic mass dependence of C and $\zeta^z_{6a,6b}$. The rotational constant C is the reciprocal of the moment of inertia about the out-of-plane axis I_z, so that the change is expected to be approximately proportional to N_D. As for $\zeta^z_{6a,6b}$, the following equation can be derived from Eqs. (3) and (6):

$$\zeta^z_{6a,6b} = \sum_n \frac{m_n}{(\mu_{6a})^{1/2}(\mu_{6b})^{1/2}} (X_{6a,n}Y_{6b,n} - Y_{6a,n}X_{6b,n}), \quad (15)$$

where μ_{6a} and μ_{6b} are the reduced masses for normal vibrations of 6a and 6b, respectively. If we assume that the displacements and reduced mass are identical for all H/D isotopomers, the difference of $\zeta^z_{6a,6b}$ between C_6H_6 and an isotopomer is approximately presented by

$$\zeta'^{\,z}_{6a,6b} - \zeta''^{\,z}_{6a,6b} = \frac{1}{(\mu_{6a})^{1/2}(\mu_{6b})^{1/2}} \times \sum_{n'} \left[\Delta m_{n'}(X_{6a,n'}Y_{6b,n'} - Y_{6a,n'}X_{6b,n'})\right]. \quad (16)$$

Here, $\zeta'^{\,z}_{6a,6b}$ and $\zeta''^{\,z}_{6a,6b}$ are the Coriolis zeta constants of a substituted molecule and of C_6H_6, respectively. n' represents the deuterated nuclei, and $\Delta m_{n'}$ is the change of nuclear mass of n' in the substitution. This indicates that the change in $\zeta^z_{6a,6b}$ by isotopomers is proportional to N_D. The $\xi^c_{6a,6b}$ value is therefore expected to depend on the square of N_D. The change in C and $\zeta^z_{6a,6b}$, however, is very small compared with their own values. It is therefore concluded that $\xi^c_{6a,6b}$ is approximately proportional to N_D. We could obtain the atomic coordinates and displacements for 6a and 6b by the vibrational calculation, explained in Section III A 1, and finally estimated the $\xi^c_{6a,6b}$ values of all isotopomers. The results are also shown in Fig. 7. These calculated values are in good agreement with the experimental ones. It should be noted that the changes in normal coordinates with isotopomers possibly affect the $\zeta^z_{6a,6b}$ value. The change in the calculated values using only the normal coordinate of C_6H_6 was significantly smaller than that using each individual normal coordinate of deuterated benzenes. Even so, it has been shown that $\zeta^z_{6a,6b}$ decreases proportionally with N_D.

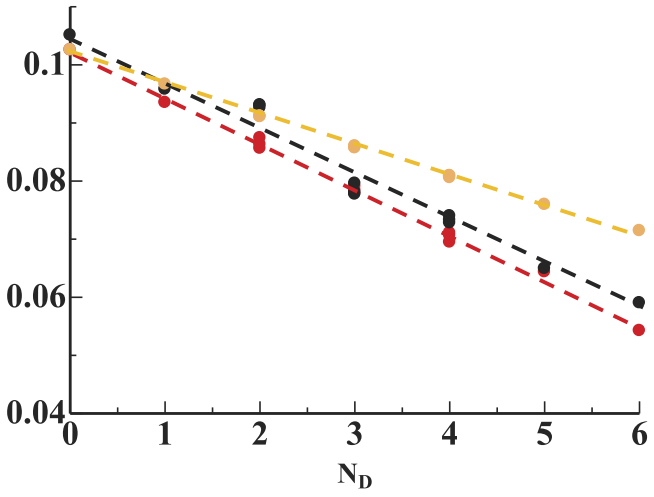

FIG. 7. N_D dependence of the Coriolis parameter, $\xi^c_{6a,6b}$. Black: $\xi^c_{6a,6b}$ (Obs.), red: $\xi^c_{6a,6b}$ (Calc.) with each Q_6, and orange: $\xi^c_{6a,6b}$ (Calc.) fixed Q_6 of C_6H_6.

The linear dependence of the Coriolis parameter on the N_D, however, is not always valid. According to the calculation using Gaussian 09, the displacement and reduced mass of 6a and 6b do not vary much by deuterium substitution. This is because the displacements of 6a and 6b consist mainly of ring deformation and do not change much by deuterium substitution. On the other hand, if we calculate the modes which contain sufficient H/D nuclei displacements, the reduced mass and displacement will be quite different by substitution and Eq. (16) does not hold.

IV. CONCLUSIONS

For all deuterated benzenes, we analyzed the vibrational and rotational structures of the $6a^1$ and $6b^1$ vibrational levels in the S_1 state. Although the two levels are degenerate in C_6H_6, C_6D_6, and 1,3,5-$C_6H_3D_3$, they are split by 2-5 cm^{-1} in other isotopomers. The results of theoretical calculation are in good agreement with our observations, and are useful to identify the observed spectral bands. The rotational constants were shown to be appreciably different between the $6a^1$ and $6b^1$ vibrational levels. We suggest that the mean molecular structures in these levels depend on their normal coordinates and anharmonicity in the potential energy. The rotational levels are shifted by Coriolis interaction between these two levels.

Spectral analysis showed that the Coriolis parameter $\xi^c_{6a,6b}$ decreased with N_D. This tendency was understood by theoretical consideration and was verified by model calculations based on the molecular structure and normal coordinates of 6a and 6b modes. The Coriolis zeta constant delicately varies with the normal coordinates.

ACKNOWLEDGMENTS

This work was supported by the Joint studies Program (2012-2014) of the Institute for Molecular Science.

APPENDIX: NUCLEAR SPIN STATISTICS

The intensity of each rotational line is proportional to the multiplicity of nuclear spin levels. H and D nuclei possess nuclear spins of $I = 1/2$ and $I = 1$, respectively, so that the multiplicity depends on the number of D atoms and substituted positions. We represent the nuclear wave function of a molecule as

$$\Psi_{nuc} = \Psi_v\Psi_r\Psi_I. \quad (A1)$$

Here, Ψ_v, Ψ_r, and Ψ_I are the vibrational, rotational and nuclear spin parts, respectively. An H nucleus is a fermion

TABLE II. Symmetry of wave functions and nuclear spin statistics of deuterated isotopomers.

	Symmetry	Ψ_I	Ψ_{nuc}	*ee*:*eo*:*oe*:*oo*	2^N3^{6-N}
C_6H_6	D_{6h}	$13A_1+A_2+7B_1+3B_2+9E_1+11E_2$	B_1		64
C_6H_5D	C_{2v}	$60A+36B$	A	5:5:3:3	96
o-$C_6H_4D_2$	C_{2v}	$78A+66B$	A	13:13:11:11	144
m-$C_6H_4D_2$	C_{2v}	$84A+60B$	B	5:7:7:5	144
p-$C_6H_4D_2$	D_{2h}	$51A_1+27B_1+27B_2+39B_3$	A_1	17:13:9:9	144
1,3,5-$C_6H_3D_3$	D_{3h}	$56A_1+20A_2+70E$	A_2		216
1,2,3-$C_6H_3D_3$	C_{2v}	$126A+90B$	B	5:7:7:5	216
1,2,4-$C_6H_3D_3$	C_s	...	...	1:1:1:1	216
o-$C_6H_2D_4$	C_{2v}	$171A+153B$	B	17:19:19:17	324
m-$C_6H_2D_4$	C_{2v}	$189A+135B$	B	5:5:7:7	324
p-$C_6H_2D_4$	D_{2h}	$99A_1+72B_1+72B_2+81B_3$	B_3	9:8:8:11	324
C_6HD_5	C_{2v}	$270A+216B$	A	5:4:4:5	486
C_6D_6	D_{6h}	$92A_1+38A_2+73B_1+46B_2+116E_1+124E_2$	A_1		729

TABLE III. Symmetry of wave functions and nuclear spin statistics of symmetric-top isotopomers (p is natural number).

Isotopomer	K_c	J	Ψ_r	Ψ_I	S_{J,K_c}
C_6H_6	$6p$		A_1+A_2	B_1+B_2	10
	$6p-5, 6p-1$		E_1	E_2	11
	$6p-4, 6p-2$		E_2	E_1	9
	$6p-3$		B_1+B_2	A_1+A_2	14
	0	$J=even$	A_1	B_1	7
		$J=odd$	A_2	B_2	3
1,3,5-$C_6H_3D_3$	$3p$		A_1+A_2	A_2+A_1	76
	$3p-1, 3p-2$		E	E	70
	0	$J=even$	A_1	A_2	20
		$J=odd$	A_2	A_1	56
C_6D_6	$6p$		A_1+A_2	A_1+A_2	130
	$6p-5, 6p-1$		E_1	E_1	116
	$6p-4, 6p-2$		E_2	E_2	124
	$6p-3$		B_1+B_2	B_1+B_2	119
	0	$J=even$	A_1	A_1	92
		$J=odd$	A_2	A_2	38

whose wave function is anti-symmetric (changes the sign with respect to exchange of the particle), while a D nucleus is a boson that has a symmetric wave function. If we consider the zero-vibrational level in the electronic ground state, Ψ_v is symmetric. The symmetry of Ψ_I, therefore, depends on Ψ_r. In Table II, the symmetries (irreducible representations) of Ψ_I and Ψ_{nuc} are listed for all deuterated benzenes. We ignore the parity here because the σ_h operation never exchanges the particles in a planar molecule. *ee*:*eo*:*oe*:*oo* represents the ratio of nuclear spin state multiplicity for the odd or even K_aK_c rotational levels. The total number of the nuclear spin states is 2^N3^{6-N}, where N is the number of H atoms.

For the symmetric-top molecules such as C_6H_6, 1,3,5-$C_6H_3D_3$, and C_6D_6, the nuclear spin statistics are somewhat complicated because Ψ_I includes E symmetry (second-order irreducible representation). The nuclear spin state multiplicity $S_{J,Kc}$ for the three isotopomers is presented in Table III. The line intensity strongly depends on the rotational quantum numbers J and K_c.

[1]C. S. Parmenter, Adv. Chem. Phys. **22**, 365 (1972).
[2]P. Avouris, W. M. Gelbart, and M. A. El-Sayed, Chem. Rev. **77**, 793 (1977).
[3]J. H. Callomon, T. M. Dunn, and I. M. Mills, Philos. Trans. R. Soc., A **259**, 499 (1966).
[4]T. Suzuki and M. Ito, J. Chem. Phys. **91**, 4564 (1989).
[5]S. Kunishige, T. Katori, M. Baba, M. Nakajima, and Y. Endo, J. Chem. Phys. **143**, 244302 (2015).
[6]H. Sieber, E. Riedle, and H. J. Neusser, J. Chem. Phys. **89**, 4620 (1988).
[7]M. Okruss, R. Müller, and A. Hese, J. Mol. Spectrosc. **193**, 293 (1999).
[8]E. Riedle, A. Beil, D. Luckhaus, and M. Quack, Mol. Phys. **81**, 1 (1994).
[9]E. B. Wilson, Jr., Phys. Rev. **45**, 706 (1934).
[10]G. Herzberg, *Molecular Spectra and Molecular Structure. II. Infrared and Raman Spectra of Polyatomic Molecules* (Van Nostrand Reinhold, New York, 1945).
[11]S. Kunishige, T. Katori, M. Kawabata, T. Yamanaka, and M. Baba, J. Chem. Phys. **143**, 244304 (2015).
[12]M. Misono, J. Wang, M. Ushino, M. Okubo, H. Katô, M. Baba, and S. Nagakura, J. Chem. Phys. **116**, 162 (2002).
[13]A. Doi, S. Kasahara, H. Katô, and M. Baba, J. Chem. Phys. **120**, 6439 (2004).
[14]A. Doi, M. Baba, S. Kasahara, and H. Katô, J. Mol. Spectrosc. **227**, 180 (2004).
[15]H. Hayashi and Y. Ohshima, Chem. Phys. **419**, 131 (2013).
[16]H. Hayashi and Y. Ohshima, J. Phys. Chem. A **117**, 9819 (2013).
[17]I. M. Mills, Pure Appl. Chem. **11**, 325 (1965).

[18]M. Oldani and A. Bauder, Chem. Phys. Lett. **108**, 7 (1984).
[19]A Program for Simulating Rotational Structure, C. M. Western, University of Bristol, 2012, http://pgopher.chm.bris.ac.uk.
[20]J. Pliva, J. W. C. Johns, and L. Goodman, J. Mol. Spectrosc. **140**, 214 (1990).
[21]M. Baba, Y. Kowaka, U. Nagashima, T. Ishimoto, H. Goto, and N. Nakayama, J. Chem. Phys. **135**, 054305 (2011).
[22]M. J. Frisch, G. W. Trucks, H. B. Schlegel, G. E. Scuseria, M. A. Robb, J. R. Cheeseman, G. Scalmani, V. Barone, B. Mennucci, G. A. Petersson, H. Nakatsuji, M. Caricato, X. Li, H. P. Hratchian, A. F. Izmaylov, J. Bloino, G. Zheng, J. L. Sonnenberg, M. Hada, M. Ehara, K. Toyota, R. Fukuda, J. Hasegawa, M. Ishida, T. Nakajima, Y. Honda, O. Kitao, H. Nakai, T. Vreven, J. A. Montgomery, Jr., J. E. Peralta, F. Ogliaro, M. Bearpark, J. J. Heyd, E. Brothers, K. N. Kudin, V. N. Staroverov, T. Keith, R. Kobayashi, J. Normand, K. Raghavachari, A. Rendell, J. C. Burant, S. S. Iyengar, J. Tomasi, M. Cossi, N. Rega, J. M. Millam, M. Klene, J. E. Knox, J. B. Cross, V. Bakken, C. Adamo, J. Jaramillo, R. Gomperts, R. E. Stratmann, O. Yazyev, A. J. Austin, R. Cammi, C. Pomelli, J. W. Ochterski, R. L. Martin, K. Morokuma, V. G. Zakrzewski, G. A. Voth, P. Salvador, J. J. Dannenberg, S. Dapprich, A. D. Daniels, O. Farkas, J. B. Foresman, J. V. Ortiz, J. Cioslowski, and D. J. Fox, GAUSSIAN 09, Revision C.01, Gaussian, Inc., Wallingford CT, 2010.